Moreno González, M.; Blasco Lanzuela, T.; Góra-Marek, K.; Palomares Gimeno, AE.; Corma Canós, A. (2014). Study of propane oxidation on Cu-zeolite catalysts by in-situ EPR and IR spectroscopies. Catalysis Today. 227:123-129. doi:10.1016/j.cattod.2013.10.055.

*Graphical Abstract (for review)

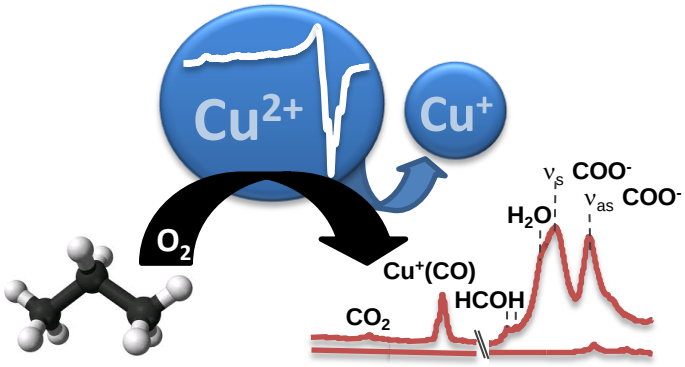

STUDY OF PROPANE OXIDATION ON Cu-ZEOLITE CATALYSTS BY IN-SITU EPR AND IR SPECTROSCOPIES

M. Moreno González,[1] T.Blasco,[1*] K. Góra-Marek,[2] A.E. Palomares,[1] A. Corma[1]

[1]*Instituto de Tecnología Química (UPV-CSIC), Universidad Politécnica de Valencia-Consejo Superior de Investigaciones Científicas, Avda. de los Naranjos s/n, 46022 Valencia (Spain)*

[2]*Faculty of Chemistry, Jagiellonian University, Ingardena 3, 30-060 Krakow (Poland)*

*Corresponding author E-mail: tblasco@itq.upv.es

Abstract

Three Cu-zeolites with different structure, Cu-TNU-9, Cu-ITQ-2 and Cu-Y have been tested as catalysts for propane oxidation reaction and the activity follows the trend: Cu-TNU-9 > Cu-ITQ-2 > Cu-Y, and *in situ* Electron Paramagnetic Resonance (EPR) and IR spectroscopies have been used to ascertain the origin of their different behavior. The IR spectra show bands ascribed to the formation of adsorbed COO^- and -CHO as reaction intermediates in the oxidation of propane. The intensity of these bands for the Cu-zeolites show the same tendency that their oxidation activity. The EPR spectra of the three Cu-zeolites show that about 40-50 % of total copper is present as isolated Cu^{2+} species, and heating under propane or propane-oxygen mixture at 350 ºC provokes the reduction of Cu^{2+} to Cu^{+} following the same trend that the oxidation activity, i.e., Cu-TNU-9 > Cu-ITQ-2 > Cu-Y. Further analysis of the EPR spectra suggests that the reducibility of exchanged Cu^{2+} cations in the Cu-zeolites is determined by their accessibility to the propane molecules.

Keywords

EPR

IR

Cu-Zeolite

Propane oxidation

SCR-NOx

Introduction

Propane is the most abundant light hydrocarbon among the organic compounds emitted from combustion of liquefied petroleum gas (LPG), used in internal combustion engines in vehicles and in stationary applications. LPG is a common fuel because it has the advantage of giving clean combustion with no soot and few sulphur emissions and of simple storage. However, the exhaust gas from LPG combustor still contains a significant amount of hydrocarbons which are hazardous to the environment [1]. In order to fulfil the demanding environmental legislations, catalytic oxidation is a promising technology for controlling organic pollutant emissions such as propane [2].

Typical catalysts for total oxidation of hydrocarbons consist of supported noble metal (Pt, Pd, Rh, Au ...) [2-6]. Alternatively, bulk metal oxides [7], mixed oxides (perovskites or hydrotalcites) [1, 8] or transition metal ion exchanged zeolites (TMI-zeolites) have been explored as catalysts, and among them, those based on copper oxide give excellent activity in combustion of volatile organic compounds (VOCs) [9-14]. Moreover, Cu-zeolites have been investigated in the last years because they exhibit high activity for NO decomposition and for NO selective catalytic reduction (NO-SCR) [15-20]. This pollutant is produced in different combustion processes such as those taking place in diesel engines, and in this case, hydrocarbons, such as propane, have been suggested to be used as a reducing agents in the NO-SCR reaction. As Cu-zeolites can catalyse both reactions, there is an intense activity on the investigation of Cu-exchanged zeolites aimed to elucidate the nature of copper active sites, their physical chemical properties and the reaction pathways.

In this work we have investigated the reaction of propane with oxygen with the aim of getting information on the mechanism of hydrocarbon oxidation on Cu-zeolites, but also as a preliminary study to understand how Cu-Zeolites catalyse the selective reduction of

NO with propane in the presence of oxygen (HC-SCR-NO). For this purpose, we have chosen three zeolites with different topologies, Cu-Y, Cu-ITQ-2 and Cu-TNU-9, as catalysts. Zeolite Y possesses FAU-type structure consisting of a three dimentional system of 12 membered rings (12 MR) channels and supercages with diameter of about 11,2 Å. ITQ-2 is the delaminated precursor of zeolite MCM-22 (MWW-type), being formed by single layers with external 12 MR cups and 10 MR channel system running in between the cups, inside the sheets. TNU-9 is a new zeolite with a structure consisting of a three dimensional channel system with pore openings of 10 MR. Here, we have employed EPR spectroscopy to study the redox properties of copper sites and follow their evolution upon heating in the presence of propane and propane-oxygen mixtures, and infrared spectroscopy to identify the intermediate species formed in the reaction of propane and oxygen. It will be shown that the ability of Cu-zeolites for propane oxidation depends on the redox properties of the copper sites.

Experimental

Zeolite TNU-9 was synthesized according to the procedure described previously [21, 22], using 1,4-bis-(N-methylpryrrolidinium)-butane and Na^+ cations as structure directing agents (SDAs). ITQ-2 was prepared by swelling the MCM-22 precursor with a water solution of hexadecyltrimethylammonium bromide and tetrapropylammonium hydroxide following the method depicted in previous publications [23, 24]. Zeolite Y is commercially available (CBV 720, Zeolyst International). Prior to ion exchange, all zeolites were rinsed with a 0,04 M solution of $NaNO_3$ in order to have the materials in the sodium form. The metal exchange was carried out by immersing the zeolite in an aqueous solution of the desired amount of $Cu(CH_3COO)_2 \cdot 4H_2O$, with a zeolite/liquid

ratio of 10 g/l and under stirring for 24 h at room temperature. The chemical composition of the samples was analyzed by ICP-O ES (Varian 715-ES), and the results are reported in Table 1.

EPR spectra were recorded with a Bruker EMX-12 spectrometer operating at the X-band, with a modulation frequency of 100 KHz and amplitude of 1.0 Gauss. All spectra were measured at -168 °C and quantitative analysis was carried out by double integration of the spectra, using $CuSO_4$ as an external standard. About 20 mg of the Cu-zeolite sample was placed into 5 mm quartz EPR tubes adapted to a high vacuum valve and dehydrated under dynamic vacuum at 500 °C for 1 h reaching a final pressure $\approx 10^{-6}$ mbar. Propane and/or oxygen were then adsorbed at -196 °C by connecting the sample tube on a vacuum line and admitting onto the Cu-zeolite the desired amount of gas using a calibrated volume. In all experiments 2 molecules propane per atom of Cu were adsorbed. In another set of experiments, an excess of oxygen, about nine molecules of oxygen per atom of Cu, was admitted into the sample tube immersed into liquid nitrogen after the adsorption of propane.

IR spectra were recorded with a Bruker Tensor 27 spectrometer (equipped with a MCT detector) with a spectral resolution of 2 cm^{-1}. Thin wafers of Cu-zeolite (5-10 mg/cm^2) were activated in the IR cell under vacuum at 500 °C for 1h, and then the adsorption of propane and/or oxygen was carried out at room temperature. Carbon monoxide (PRAXAIR 9.5) was used as a probe molecule.

Catalytic tests were carried out in a fixed bed, quartz tubular reactor. In the C_3H_8 oxidation experiments, 66.7 mg of catalyst, as particles of 0.25-0.42 mm size, were introduced in the reactor, heated up to 500 ºC under nitrogen flow and kept at this temperature for 30 minutes. After that, the desired temperature was set and the flow changed to the reaction feed consisting of 500 $ml.min^{-1}$ of a mixture composed by

0.33% C_3H_8, 6.9% O_2 and N_2 as gas balance. The reaction was followed by the CO_2 formed that was analysed with a non-dispersive infrared detector Servomex 4900.

Results and discussion

Table 1 shows the chemical composition and the level of copper exchange of the Cu-TNU-9, Cu-Y and Cu-ITQ-2 zeolites used in this work, as well as the conversion of propane to CO_2 in the oxidation reaction at 350 ºC. This temperature is within the range typical for total oxidation and for SCR-NO reactions. As it can be observed in Table 1, the three Cu-zeolites display a very different conversion being the highest for Cu-TNU-9 and the lowest for Cu-Y, with an intermediate value for Cu-ITQ-2. In order to rationalize the different catalytic activity of these Cu-zeolites we have combined EPR and infrared spectroscopy. The EPR and infrared spectra of Cu-zeolites were acquired after gas adsorption, and then after subsequent heating in an external oven at 350 ºC.

EPR Spectroscopy

EPR spectroscopy allows the detection of paramagnetic Cu^{2+} cations with a d^9 electronic configuration, although only isolated Cu^{2+} are observed because the dipolar coupling among paramagnetic cations in aggregated species inhibit the observation of any EPR signal. The interaction of the magnetic moments associated with the unpaired electron of Cu^{2+} with the nuclear spin I=3/2 of the two copper isotopes, ^{63}Cu and ^{65}Cu with natural abundance 69.15 % and 30.85 %, respectively, gives rise to a hyperfine structure consisting of four lines. The EPR signals of Cu^{2+} in Cu-zeolites are usually axially symmetric and the hyperfine structure is better resolved in the low field region of the spectra, corresponding to the parallel component.

The EPR spectra of the Cu-zeolites studied here under ambient conditions (not shown) consist of an axially symmetric signal of octahedral Cu^{2+} resulting from the coordination to six H_2O molecules, or more probable to H_2O and oxygen atoms of the zeolite framework $[CuO_x(H_2O)_{6-x}]^{2+}$ [25-33]. According to the quantification of the paramagnetic signals, isolated Cu^{2+} species accounts for 40-50 % of total in the three Cu-zeolites, indicating that about half of copper is EPR silent and must be in the form of small CuO particles not detected by X-ray diffraction, or of Cu^{2+}–O–Cu^{2+} dimmers [34-36]. Prior to gas adsorption, samples were degassed at 500 ºC under high vacuum, which produced a strong decreases in the Cu^{2+} detected by EPR, to around 10 % of total, indicating that most Cu^{2+} has been reduced to diamagnetic Cu^{+}. These data are shown in Figure 1, which represent the amount of Cu^{2+} respect total copper content detected in the EPR spectra of Figures 2-4 recorded after submitting zeolites Cu-TNU-9, Cu-Y and Cu-ITQ-2 to different treatments. The parallel region of the spectra is magnified on the right part of Figures 2-4.

Figure 2a shows the EPR spectrum of zeolite Cu-TNU-9 evacuated at 500 ºC, which is formed by the superimposition of two axially symmetric signals, A and B, of isolated Cu^{2+}. The $g_{\perp}$, and $g_{//}$ and $A_{//}$ determined from the analysis of the expanded spectral region of Figure 2a right, are summarized in Table 2. To our knowledge, this is the first EPR study of zeolite Cu-TNU-9 and the assignment of signals of spectrum 2A to specific copper sites requires deeper investigation, which is out of the scope of this manuscript. Nevertheless, from comparison of the parameters shown in Table 2 with those reported in the bibliography for other Cu^{2+} exchanged zeolites [37], signals A and B can be attributed to Cu^{2+} in square pyramidal and square planar configurations, respectively. Figure 2b displays the spectrum recorded after the adsorption 2 molecules of C_3H_8 per Cu atom on Cu-TNU-9. Inspection of the low field region of the spectrum,

Figure 2b right, shows the appearance of a new signal C characterized by the parameters listed in Table 2, which must come from the interaction of Cu^{2+} with propane (Cu^{2+}-C_3H_8). Although the spectrum of Figure 2b is clearly dominated by signal C, there may be some contribution of signal B and, in any case, it is difficult to rule out the presence of signals A and B. After subsequent heating at 350 ºC, a sharp intensity decrease (see multiplication factor in the spectrum of Figure 2b) of the EPR spectrum is observed due to the reduction of Cu^{2+} to diamagnetic Cu^{+}. Interestingly, only signal A remains in the spectrum, indicating that Cu^{2+} in square planar coordination (signal B) is more reducible, probably because its easier accessibility to propane molecules due to the lower coordination number. The spectrum recorded after the co-adsorption of propane and oxygen on zeolite Cu-TNU-9, shown in Figure 2d, is only slightly broader than that of Figure 2b, suggesting that the Cu^{2+} interacts preferably with propane. Subsequent heating at 350 ºC the Cu-TNU-9 zeolite with the mixture propane/oxygen decreases the intensity of the Cu^{2+} signals but to lesser extent than in the absence of oxygen (see Figures 1 and 2d), and provokes the disappearance of signals A and B and the appearance of a new signal D due to hydrated Cu^{2+} in octahedral coordination, and a second signal C', whose parameters are collected in Table 2. The $g_{//}$ (2.372) and $A_{//}$ (131 Gauss) values of signal D are smaller than those of the EPR signal of Cu^{2+} sites in the hydrated Cu-TNU-9 zeolite ($g_{//}$ = 2,383 and $A_{//}$ = 138 Gauss), strongly suggesting that in the treated sample Cu^{2+} is coordinated to less water molecules and to more framework oxygen atoms of the zeolite [25, 38]. The formation of this $[CuO_y(H_2O)_{6-y}]^{2+}$ complex points out that water must have been produced upon heating, probably by oxidation of propane. The parameters of signal C', typical of Cu^{2+} in square pyramidal coordination, are very close to those of signal C (see Table 2) and then must be

originated by the interaction of paramagnetic Cu^{2+} with and intermediate reaction product, in agreement with the results obtained by infrared spectroscopy (vide infra).

Figure 3 shows the EPR spectra of zeolite Cu-Y submitted to treatments similar to zeolite Cu-TNU-9. The spectrum of the sample degassed at 500 ºC, displayed in Figure 3a, consists of two axially symmetric signals E and F, characterized by the parameters listed in Table 3. Signals E and F have been previously assigned to Cu^{2+} located at two different exchange positions of the FAU type zeolite [29, 30, 39-42], or at sites containing different number of Al atoms in their close environment [43]. Assuming different location, signal E has been attributed to Cu^{2+} at the six member ring of SII site in the supercage [40, 41] or at SI' within the sodalite cage [29, 30], and signal F to Cu^{2+} at SI' [40, 41] or at SI sites inside the D6R [29, 30]. Adsorption of propane on zeolite Cu-Y does not modifies the spectrum of the dehydrated zeolite (spectrum not shown), while subsequent heating at 350 ºC produces an intensity decrease (see Figure 3b) due to the reduction of Cu^{2+} to Cu^{+}, although less than for zeolite Cu-TNU-9 (see Figure 1). The spectrum 3b is dominated by signal F, indicating that the species associated to signal E have been reduced probably because their easier accessibility to propane molecules. Then, signal E must be originated by Cu^{2+} species located at SII sites in the supercage, or alternatively inside the sodalite cages (site SI´), which move to accessible supercage positions upon heating. Figure 3c shows the spectrum recorded after co-adsorption of propane and oxygen on zeolite Cu-Y. The EPR signals of Cu^{2+} are broadened because of the dipolar interaction with paramagnetic oxygen molecules, making difficult the identification of the Cu^{2+} species. Comparison with the spectrum of Figure 2d suggests a stronger interaction with oxygen than in zeolite Cu-TNU-9. Indeed, when Cu-Y is heated at 350 ºC with the propane-oxygen mixture, the overall intensity of the EPR spectrum (Figure 3d) increases indicating that, opposite to the

results obtained for Cu-TNU-9, copper has been oxidized. Despite the low resolution, analysis of the spectrum suggests the presence signals E and F.

Figure 4 shows the EPR spectra of zeolite Cu-ITQ-2 evacuated at 500 ºC (Fig. 4a), and heated at 350 ºC with propane (Fig. 4b) or with propane/oxygen (Fig. 4c), and Table 4 collects the spectral parameters of the corresponding Cu^{2+} signals. The dehydrated Cu-ITQ-2 zeolite shows the presence of three axially symmetric Cu^{2+} signals, G, H and J. We have not found any publication reporting EPR results of Cu-ITQ-2 zeolites. However, since ITQ-2 is obtained by de-lamination of the MCM-22 zeolite precursor, we have made a tentative attribution of the signals detected here by analogy to previous assignments made for Cu-MCM-22 [44-46]. Accordingly, signals G and H are attributed to Cu^{2+} species in square pyramidal coordination and signal J to Cu^{2+} in square planar symmetry. Propane adsorption produces only subtle modifications in the spectrum of the evacuated sample (not shown), and after subsequent heating, the intensity of the spectrum decreases and consists mainly of signal H, indicating some reduction to Cu^{+}, especially of species J and G (see Figure 4b). Heating zeolite Cu-ITQ-2 under propane-oxygen produces the spectrum of Figure 4c, with intensity and shape similar to that of Figure 4a for the evacuated zeolite, but with the signals shifted. Indeed the spectrum consists of two new signals K and L, characterized by the parameters listed in Table 4. Although the interpretation of spectrum 4c is not straight forward, signal K can be attributed to Cu^{2+} bonded to water molecules, based on the similarity of its parameters with those of signal D (Table 2). Meanwhile, the parameters of signal L are close to those of signal H and then can be tentatively attributed to Cu^{2+} in square pyramidal coordination in slightly different environment which may be due to the interaction with reaction intermediates.

Comparison of the results shown in Figures 2-4 and the intensity of the Cu^{2+} EPR signals depicted in Figure 1 evidences different reducibility of Cu^{2+} in Cu-TNU-9, Cu-Y and Cu-ITQ-2 zeolites when they are heated at 350 ºC in the presence of propane and propane/oxygen. When propane is used, the EPR signals intensity decreases due to the reduction of Cu^{2+} to Cu^{+}, and the amount of Cu^{2+} detected by EPR follows the trend: Cu-Y > Cu-ITQ-2 > Cu-TNU-9. The higher degree of copper reduction is attained in CuTNU-9, which takes place even in the presence of O_2, whereas heating with propane-oxygen oxidizes Cu^{+} to Cu^{2+} in zeolite Cu-Y. Meanwhile, an intermediate situation is observed for zeolite Cu-ITQ-2, as the intensity of isolated Cu^{2+} does not change significantly when the sample is heated at 350 ºC with a mixture of propane-oxygen

Infrared Spectroscopy

Figure 5 shows the infrared spectra recorded at room temperature of zeolites Cu-TNU-9, Cu-ITQ-2 and Cu-Y, after being heated at 350 ºC for 30 min with a mixture propane/oxygen, and the spectra of propane adsorbed on these same zeolites for comparison purposes. After heating under propane-oxygen mixture, the spectrum recorded for zeolite Cu-TNU-9 shows very intense bands in the 1650-1450 cm^{-1} frequency region, which are weaker for Cu-ITQ-2, and negligible for zeolite Cu-Y. The 1580 and 1480 cm^{-1} bands are characteristic of symmetric and antisymmetric stretching vibrations of the COO^{-} group ($\nu_s COO^{-}$ and $\nu_{as} COO^{-}$) [47, 48], and the small bands in the region 1750-1690 cm^{-1} can be originated from formaldehyde bonded to bridging hydroxyls groups (1750 cm^{-1}) [47, 49] or interacting with Cu^{+} sites (1690 cm^{-1}) [50]. The presence of the absorption bands typical of COO^{-} and -CHO groups points to a straightforward catalytic oxidation of the adsorbed propane by oxygen to acetates/formates or/and other oxygen containing compounds (formaldehyde).

Oxidation of propane is also manifested by the appearance of new bands at 2346 cm^{-1}, 2157 cm^{-1} and 1620 cm^{-1}. The band at 2157 cm^{-1} is typical of $Cu^{+}(CO)$ monocarbonyl [51, 52] formed by the interaction of Cu^{+} with CO coming from the partial oxidation of propane, whereas the bands at 2346 cm^{-1} (CO_2) and 1620 cm^{-1} (H_2O) confirms the total oxidation of propane. The band at 2137 cm^{-1} is assigned to CO bonded to Cu^{+} cations coordinating water molecules, which are downshifted respect the $Cu^{+}(CO)$ band (in the range 2157 - 2137 cm^{-1}) because of the electron flow from the electron donor water molecule in $(H_2O)Cu^{+}(CO)$ complexes [53]. The detection of hydrated copper species by IR agrees with the observation of hydrated $[CuO_y(H_2O)_{6-y}]^{2+}$ complexes by EPR in zeolites Cu-TNU-9 and Cu-ITQ-2. Therefore the oxidation of propane in the presence of O_2 produces H_2O molecules which coordinate to both Cu^{+} and Cu^{2+} cations. Since only CO_2 has been observed as reaction product, the oxygenate species observed by infrared spectroscopy can be considered as intermediate products in the oxidation reaction.

Figure 6 shows the infrared spectra of the Cu-zeolites submitted to the same treatment (heating with the propane/oxygen at 350 ºC) but recorded by cooling the IR cell down to -20 ^{o}C to adsorb all reaction products. This experiment was carried out to check if the amount of final product, carbon dioxide, formed under the experimental conditions used for in situ IR agrees with the catalytic results reported in Table 1. The spectra of Figure 6 show that the intensity of the CO_2 band at 2350 cm^{-1} is very weak for Cu-Y, while it is remarkable for zeolite Cu-TNU-9 and intermediate for Cu-ITQ-2. Consequently, the activity towards propane oxidation under these reaction conditions is in good agreement with the propane conversion obtained in the catalytic tests included in Table 1. Judging from the comparison of Figures 5 and 6, the intensity of the acetate/formate (1580 and 1480 cm^{-1}) infrared bands are directly related with the CO_2

production and then with the catalytic activity for the oxidation of propane of the Cu-zeolites studied here. From the high intensity of acetate/formate bands we can conclude that the propane molecules are most effectively oxidized on Cu-TNU-9 zeolite. Meanwhile the intensity of these bands is moderate for Cu-ITQ-2 and negligible for Cu-Y zeolites in agreement with their intermediate and low activity for propane oxidation.

Figure 7 shows the IR spectra obtained after CO adsorption on Cu-TNU-9 evacuated at 500 ºC and heated at 350 ºC under propane (spectrum 7a) or propane-O_2 mixture (spectrum 7b). The spectrum 7a consists of only a band at 2157 cm^{-1} of Cu^{+}(CO) monocarbonyl species, while a weak IR band of Cu^{2+}(CO) at 2206 cm^{-1} is evident in the spectrum of Figure 7b when also oxygen is present during heating. This result is in good agreement with the relative intensity of Cu^{2+} signals in the EPR spectra of the Cu-TNU-9 zeolite heated with propane and with propane-oxygen (see Figure 1).

General remarks

Despite differences in experimental conditions imposed by the use of *in situ* cells appropriate for each spectroscopy, there is a good agreement in the main conclusions reached by IR and EPR spectroscopies and the catalytic tests. According to the results reported in Table 1, and the infrared spectra of Figure 6, the catalytic activity for the oxidation of propane with oxygen at 350 ºC follows the trend: Cu-TNU-9 > Cu-ITQ-2 > Cu-Y. A similar trend is encountered for the reducibility of Cu^{2+} cations upon heating these Cu-zeolites with propane or propane-oxygen. The highest oxidation activity of Cu-TNU-9 is accompanied by the higher degree of reduction when heated under propane or propane-oxygen, as reflected by the decrease of the Cu^{2+} EPR signal (see Figure 1). On the opposite, Cu-Y show very low activity for propane oxidation and the

intensity of the Cu^{2+} EPR signal decreases slightly when heated under propane, and even increase when heating upon propane-oxygen.

The different activity of zeolites Cu-TNU-9, Cu-ITQ-2 and Cu-Y for propane oxidation (see table 1) cannot be explained by differences in the Cu content or the degree of aggregation of Cu^{2+}, but as mentioned above, there is a correlation with the extent of reduction of the isolated Cu^{2+}. Analysis of the EPR spectra strongly suggests that the reducibility of copper cations mostly depends on their accessibility to the propane molecules, and then on the distribution of Cu^{2+} in the zeolite. Accordingly, the EPR signals of Cu^{2+} in zeolite Cu-TNU-9, the most active for propane oxidation, are strongly modified by the adsorption of propane, whereas no changes are observe in the EPR spectrum of Cu-Y. Indeed, the EPR results indicate that Cu^{2+} in Cu-Y is located inside the small cages (sodalite and/or hexagonal prisms) or in non-accessible position near the 6MR between the sodalite and supercage. Nevertheless, the intensity of the EPR signal of Cu^{2+} decreases when CuY is heated under propane, probably because thermal treatment favors migration of copper to accessible position producing some reduction of Cu^{2+} ions.

Finally, we must note that although the correlation between the catalyst activity and the copper reducibility suggest that isolated Cu^{2+} are active sites for propane oxidation, we cannot discard the contribution of aggregated copper species (CuO or Cu-O-Cu dimmers) as active sites for the reaction.

To summarize, the results reported here suggest that the catalytic activity for propane oxidation to CO_2, which follows the trend Cu-TNU-9 > Cu-ITQ-2 > Cu-Y, depends on the reducibility of Cu^{2+} cations at exchange position, which is determined by its accessibility to propane molecules. Meanwhile, *in situ* IR spectroscopy shows that adsorbed formate/aldehyde species are reaction intermediates formed during oxidation.

Acknowledgements

The authors acknowledge the financial support from the Spanish Ministry of Economy and Competitiveness through the Severo Ochoa program (SEV-2012-0267) as well as operating grants Consolider Ingenio Multicat (CSD-2009-00050) and MAT-2012-3856-C02-01.

References

[1] Z. Jiang, L. Kong, Z. Chu, L.J. France, T. Xiao and P.P. Edwards, Fuel, 96 (2012) 257.

[2] M.N. Taylor, W. Zhou, T. Garcia, B. Solsona, A.F. Carley, C.J. Kiely and S.H. Taylor, Journal of Catalysis, 285 (2012) 103.

[3] O.R. Inderwildi and S.J. Jenkins, Chemical Society Reviews, 37 (2008) 2274.

[4] S. Scirè and L.F. Liotta, Applied Catalysis B: Environmental, 125 (2012) 222.

[5] X. Wu, L. Zhang, D. Weng, S. Liu, Z. Si and J. Fan, Journal of Hazardous Materials, 225–226 (2012) 146.

[6] Z. Zhu, G. Lu, Y. Guo, Y. Guo, Z. Zhang, Y. Wang and X.-Q. Gong, ChemCatChem, (2013) n/a.

[7] B. Solsona, T. Garcia, S. Agouram, G.J. Hutchings and S.H. Taylor, Applied Catalysis B: Environmental, 101 (2011) 388.

[8] N.A. Merino, B.P. Barbero, P. Grange and L.E. Cadús, Journal of Catalysis, 231 (2005) 232.

[9] R. Bulánek, B. Wichterlová, Z. Sobalík and J. Tichý, Applied Catalysis B: Environmental, 31 (2001) 13.

[10] Z. Chajar, M. Primet and H. Praliaud, Journal of Catalysis, 180 (1998) 279.

[11] A.K. Neyestanaki, N. Kumar and L.-E. Lindfors, Fuel, 74 (1995) 690.

[12] K. Alexopoulos, M. Anilkumar, M.-F. Reyniers, H. Poelman, S. Cristol, V. Balcaen, P.M. Heynderickx, D. Poelman and G.B. Marin, Applied Catalysis B: Environmental, 97 (2010) 381.

[13] V. Balcaen, H. Poelman, D. Poelman and G.B. Marin, Journal of Catalysis, 283 (2011) 75.

[14] P.M. Heynderickx, J.W. Thybaut, H. Poelman, D. Poelman and G.B. Marin, Journal of Catalysis, 272 (2010) 109.

[15] M. Iwamoto, H. Yahiro, K. Tanda, N. Mizuno, Y. Mine and S. Kagawa, The Journal of Physical Chemistry, 95 (1991) 3727.

[16] Y. Traa, B. Burger and J. Weitkamp, Microporous and Mesoporous Materials, 30 (1999) 3.

[17] V.A. Sadykov, V.V. Lunin, V.A. Matyshak, E.A. Paukshtis, A.Y. Rozovskii, N.N. Bulgakov and J.R.H. Ross, Kinetics and Catalysis, 44 (2003) 379.

[18] S. Brandenberger, O. Kröcher, A. Tissler and R. Althoff, Catalysis Reviews, 50 (2008) 492.

[19] C. Franch-Martí, C. Alonso-Escobar, J.L. Jorda, I. Peral, J. Hernández-Fenollosa, A. Corma, A.E. Palomares, F. Rey and G. Guilera, Journal of Catalysis, 295 (2012) 22.

[20] U. Deka, I. Lezcano-Gonzalez, B.M. Weckhuysen and A.M. Beale, ACS Catalysis, 3 (2013) 413.

[21] S.B. Hong, E.G. Lear, P.A. Wright, W. Zhou, P.A. Cox, C.-H. Shin, J.-H. Park and I.-S. Nam, Journal of the American Chemical Society, 126 (2004) 5817.

[22] S.B. Hong, H.-K. Min, C.-H. Shin, P.A. Cox, S.J. Warrender and P.A. Wright, Journal of the American Chemical Society, 129 (2007) 10870.

[23] A. Corma, V. Fornes, S.B. Pergher, T.L.M. Maesen and J.G. Buglass, Nature, 396 (1998) 353.

[24] A. Corma, V. Fornés, J.M. Guil, S. Pergher, T.L.M. Maesen and J.G. Buglass, Microporous and Mesoporous Materials, 38 (2000) 301.

[25] M.W. Anderson and L. Kevan, The Journal of Physical Chemistry, 91 (1987) 4174.

[26] S.C. Larsen, A. Aylor, A.T. Bell and J.A. Reimer, The Journal of Physical Chemistry, 98 (1994) 11533.

[27] S.-K. Park, V. Kurshev, Z. Luan, C. Wee Lee and L. Kevan, Microporous and Mesoporous Materials, 38 (2000) 255.

[28] J. Xu, J.-S. Yu, S.J. Lee, B.Y. Kim and L. Kevan, The Journal of Physical Chemistry B, 104 (2000) 1307.

[29] J.S. Yu and L. Kevan, The Journal of Physical Chemistry, 94 (1990) 7612.

[30] T. Ichikawa and L. Kevan, The Journal of Physical Chemistry, 87 (1983) 4433.

[31] H. Yahiro, Y. Ohmori and M. Shiotani, Microporous and Mesoporous Materials, 83 (2005) 165.

[32] J. Wang, T. Yu, X. Wang, G. Qi, J. Xue, M. Shen and W. Li, Applied Catalysis B: Environmental, 127 (2012) 137.

[33] M. Zamadics, X. Chen and L. Kevan, The Journal of Physical Chemistry, 96 (1992) 2652.

[34] F.X. Llabrés i Xamena, P. Fisicaro, G. Berlier, A. Zecchina, G.T. Palomino, C. Prestipino, S. Bordiga, E. Giamello and C. Lamberti, The Journal of Physical Chemistry B, 107 (2003) 7036.

[35] G.T. Palomino, P. Fisicaro, S. Bordiga, A. Zecchina, E. Giamello and C. Lamberti, The Journal of Physical Chemistry B, 104 (2000) 4064.

[36] J.Y. Yan, G.D. Lei, W.M.H. Sachtler and H.H. Kung, Journal of Catalysis, 161 (1996) 43.

[37] A. Delabie, K. Pierloot, Marijke H. Groothaert, Robert A. Schoonheydt and Luc G. Vanquickenborne, European Journal of Inorganic Chemistry, 2002 (2002) 515.

[38] M. Zamadics, X. Chen and L. Kevan, The Journal of Physical Chemistry, 96 (1992) 5488.

[39] D. Berthomieu, J.-M. Ducéré and A. Goursot, The Journal of Physical Chemistry B, 106 (2002) 7483.

[40] R.A. Schoonheydt, Catalysis Reviews, 35 (1993) 129.

[41] J.C. Conesa and J. Soria, Journal of the Chemical Society, Faraday Transactions 1: Physical Chemistry in Condensed Phases, 75 (1979) 406.

[42] D. Berthomieu, J.M. Ducéré and A. Goursot, in G.G. R. Aiello and F. Testa (Editors), Studies in Surface Science and Catalysis, Vol. Volume 142, Elsevier, 2002, p. 1899.

[43] K. Pierloot, A. Delabie, M. Groothaert and R. Schoonheydt, Phys. Chem. Chem. Phys., 3 (2001) 2174.

[44] P. Kaminski, I. Sobczak, P. Decyk, M. Ziolek, W.J. Roth, B. Campo and M. Daturi, The Journal of Physical Chemistry C, 117 (2013) 2147.

[45] M. Milanesio, G. Croce, D. Viterbo, H.O. Pastore, A.J.d.S. Mascarenhas, E.C.d.O. Munsignatti and L. Meda, The Journal of Physical Chemistry A, 112 (2008) 8403.

[46] T. Wasowicz, A.M. Prakash and L. Kevan, Microporous Materials, 12 (1997) 107.

[47] E. Kukulska-Zając, K. Góra-Marek and J. Datka, Microporous and Mesoporous Materials, 96 (2006) 216.

[48] M. Davies, Elsevier, Amsterdam/London/New York, (1963) 419.

[49] K. Góra-Marek, Microporous and Mesoporous Materials, 145 (2011) 93.

[50] E. Kukulska-Zając and J. Datka, The Journal of Physical Chemistry C, 111 (2007) 3471.

[51] G. Hubner, G. Rauhut, H. Stoll and E. Roduner, Physical Chemistry Chemical Physics, 4 (2002) 3112.

[52] G.T. Palomino, S. Bordiga, A. Zecchina, G.L. Marra and C. Lamberti, The Journal of Physical Chemistry B, 104 (2000) 8641.

[53] K. Góra-Marek, Vibrational Spectroscopy, 58 (2012) 104.

Figures Caption

Figure 1: Intensity of EPR signals expressed as the percentage of Cu (II) detected by EPR respect to the copper content determined by chemical analysis, after the treatment indicated in the Figure.

Figure 2: EPR spectra at -168 ºC of Cu-TNU-9 catalyst evacuated at 500 ºC (a) and then after propane adsorption (2 molecules of C_3H_8 per atom of Cu) (b) and subsequent heating at 350 ºC for 30 minutes (c); and after adsorption 2 molecules of C_3H_8 and 12 of O_2 per atom of Cu (d) and subsequent heating at 350 ºC for 30 minutes (e). On the right: magnification of the low-field hyperfine features of the normalized EPR spectra.

Figure 3: EPR spectra at -168 ºC of Cu-Y catalyst evacuated at 500 ºC (a) and then after propane adsorption (2 molecules of C_3H_8 per atom of Cu) and heating at 350 ºC 30 min (b); after adsorption of 2 molecules of C_3H_8 and 15 of O_2 per atom of Cu (c) and subsequently heating at 350 ºC 30 min (d). On the right: magnification of the low-field hyperfine features of the normalized EPR spectra.

Figure 4: EPR spectra at -168 ºC of Cu-ITQ-2 catalyst evacuated at 500 ºC (a) and then after propane adsorption (2 molecules of C_3H_8 per atom of Cu) and heating at 350 ºC for 30 minutes (b); and after adsorption of 2 molecules of C_3H_8 and 9 of O_2 per atom of Cu and heating at 350 ºC for 30 minutes (c). On the right: magnification of the low-field hyperfine features of the normalized EPR spectra.

Figure 5: IR spectra of Cu-TNU-9 (a), Cu-ITQ-2 (b) and Cu-Y (c) zeolites recorded after adsorption of propane (a, b, c) and after heating at 350 ºC for 30 minutes in the presence of propane and oxygen (a´, b´, c´).

Figure 6. IR spectra of CO_2 produced during heating with propane/oxygen mixture at 350 ºC. Spectrum was collected at -20 ºC.

Figure 7. IR spectra of CO adsorbed on CuTNU-9 catalyst evacuated at 500 ºC: after heating with propane at 350 ºC (a) and after heating with propane/oxygen mixture at 350 ºC (b). Carbon monoxide was sorbed at -150 ºC.

Table 1

Chemical composition of the Cu-zeolites used in this study and the propane conversion to CO_2 in the oxidation reaction.

Catalyst	wt % Cu	Si/Al	Cu/Al	% Exchange	% Conversion
Cu-Y	3,29	11	0,47	94	10
Cu-ITQ-2	2,74	20	0,62	123	40
Cu-TNU-9	4,16	14	0,67	135	85

Table 2

EPR parameters of the Cu^{2+} signals of zeolite Cu-TNU-9 submitted to different treatments corresponding to the spectra displayed in Figure 2.

Treatment	Signal	EPR parameters			Cu^{2+} species
		A_{II}/Gauss	g_{II}	$g_{\perp}$	
Evac at 500 ºC	A	163	2,303	2,058	$Cu^{2+}_{sq\text{-}pyr}$
	B	171	2,282	-	$Cu^{2+}_{sq\text{-}pl}$
$2C_3H_8$/Cu	C	155	2,318	2,048	Cu^{2+}-C_3H_8
$2C_3H_8$/Cu T_{reac}=350 ºC	A	161	2,316	2,059	$Cu^{2+}_{sq\text{-}pyr}$
$2C_3H_8/12O_2$/Cu T_{reac}=350 ºC	D	131	2,372	2,078	Cu^{2+}-H_2O
	C’	156	2,325	2,048	Cu^{2+}-$C_xH_yO_z$

Table 3

EPR parameters of the Cu^{2+} signals of zeolite Cu-Y submitted to different treatments, corresponding to the spectra displayed in Figure 3.

Treatment	Signal	EPR parameters			Cu^{2+} species
		A_{II}/Gauss	g_{II}	$g_{\perp}$	
Evac at 500 ºC	E	127	2,380	2,060	SII/SI'
	F	157	2,330	-	SI'/SI
$2C_3H_8$/Cu T_{reac}=350 ºC	F	157	2,330	2,059	SI'/SI
$2C_3H_8/15O_2$/Cu T_{reac}=350 ºC	E	127	2,380	2,060	SII/SI'
	F	157	2,314	-	SI'/SI

Table 4

EPR parameters of the Cu^{2+} signals of zeolite Cu-ITQ-2 submitted to different treatments, corresponding to the spectra displayed in Figure 4.

Treatment	Signal	EPR parameters			Cu^{2+} species
		A_{II}/Gauss	g_{II}	$g_{\perp}$	
Evac at 500 ºC	G	139	2,355	2,043	$Cu^{2+}_{sq\text{-}pyr}$
	H	161	2,333	-	$Cu^{2+}_{sq\text{-}pyr}$
	J	167	2,280	-	$Cu^{2+}_{sq\text{-}pl}$
$2C_3H_8$/Cu T_{reac}=350 ºC	H	157	2,329	2,060	$Cu^{2+}_{sq\text{-}pyr}$
$2C_3H_8/12O_2$/Cu T_{reac}=350 ºC	K	132	2,374	2,061	Cu^{2+}-H_2O
	L	157	2,340	-	Cu^{2+}-$C_xH_yO_z$

Figure

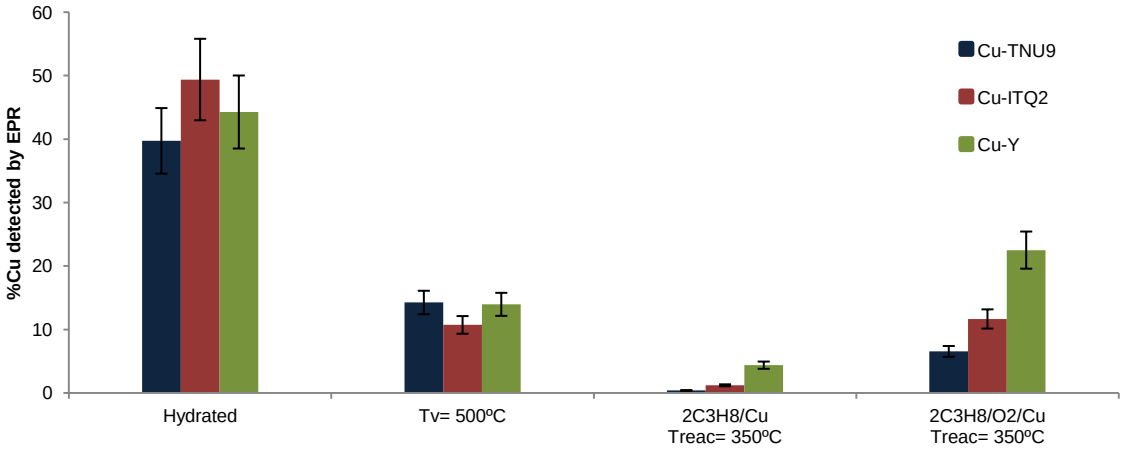

Figure 1

Figure

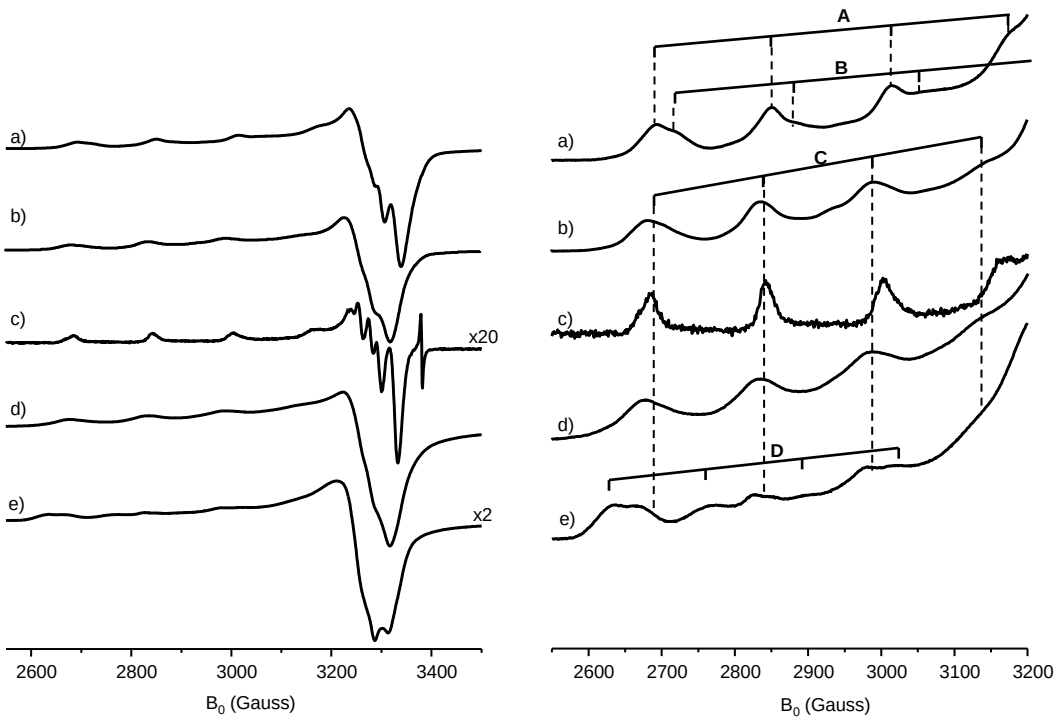

Figure 2

Figure

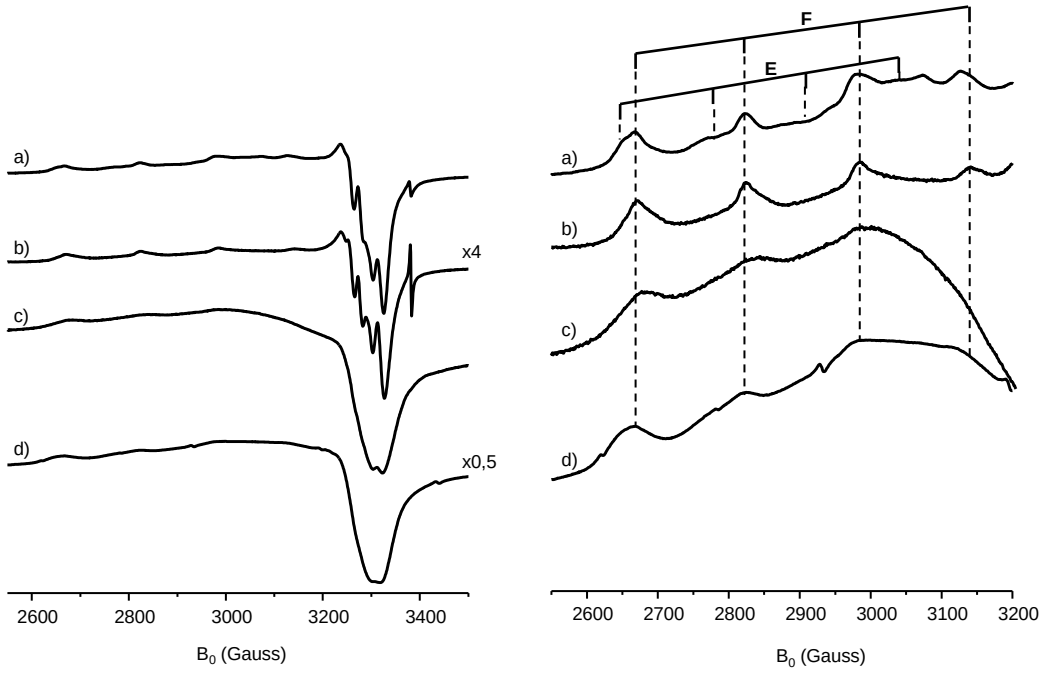

Figure 3

Figure

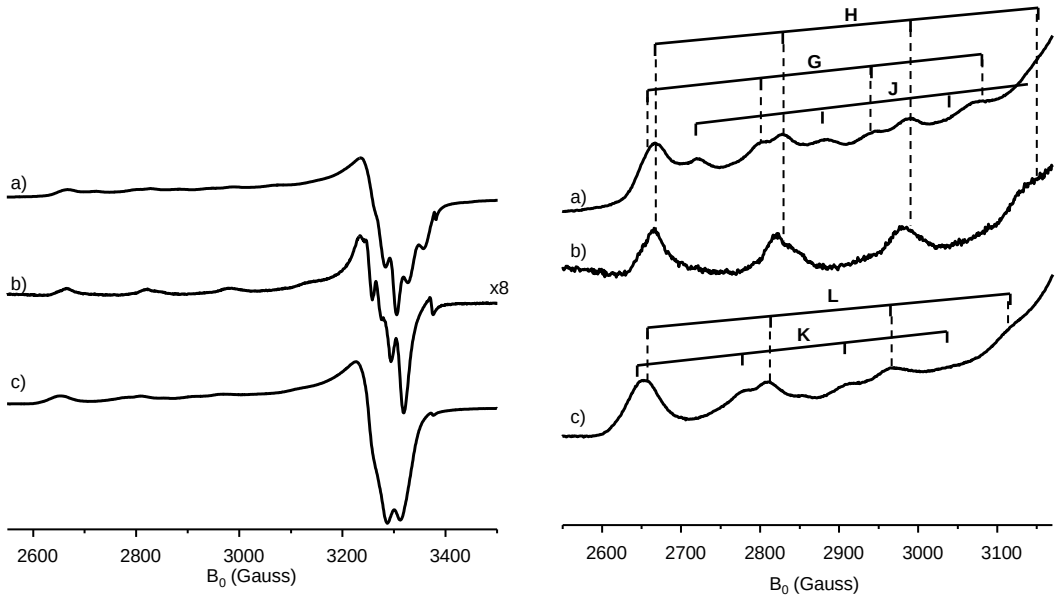

Figure 4

Figure

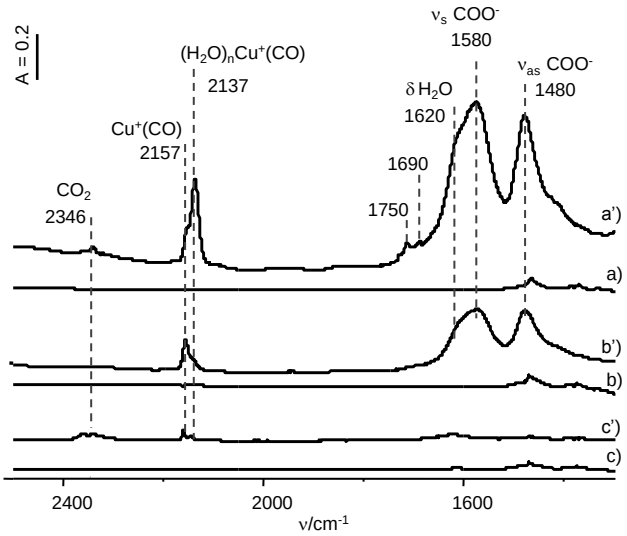

Figure 5

Figure

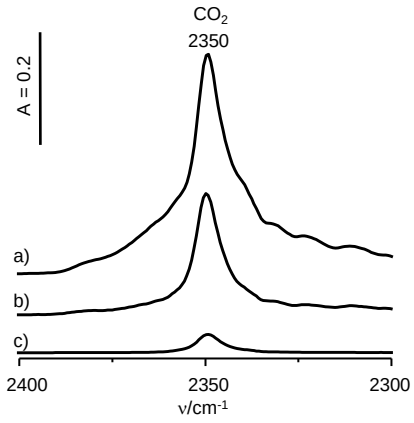

Figure 6

Figure

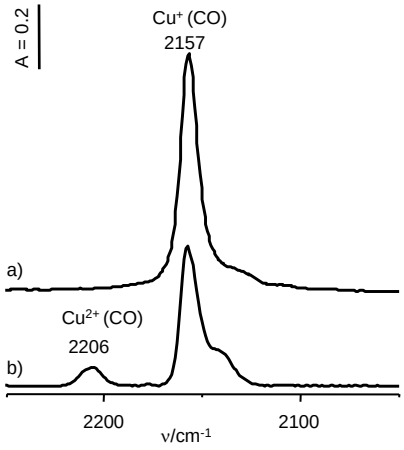

Figure 7